

# Nature Inspired Phenotype Analysis with 3D Model Representation Optimization

Lu Cao and Fons J. Verbeek

Section Imaging & BioInformatics, Leiden Institute of Advanced Computer Science,  
Leiden University, Leiden, The Netherlands  
luca@liacs.nl, fverbeek@liacs.nl

**Abstract.** In biology 3D models are made to correspond with true nature so as to use these models for a precise analysis. The visualization of these models helps in the further understanding and conveying of the research questions. Here we use 3D models in gaining understanding on branched structures. To that end we will make use of L-systems and will attempt to use the results of our analysis for the gaining of understanding of these L-systems. To perform our analysis we will have to optimize the 3D models. There are lots of different methods to produce such 3D model. For the study of micro-anatomy, however, the possibilities are limited. In planar sampling, the resolution in the sampling plane is higher than the planes perpendicular to the sampling plane. Consequently, 3D models are under sampled along, at least, one axis. In this paper we present a pipeline for reconstruction of a stack of images. We devised a method to convert the under sampled stack of contours into a uniformly distributed point cloud. The point cloud as a whole is integrated in construction of a surface that accurately represents the shape. In the pipeline the 3D dataset is processed and its quality gradually upgraded so that accurate features can be extracted from under sampled dataset.

The optimized 3D models are used in the analysis of phenotypical differences originating from experimental conditions by extracting related shape features from the model. We use two different sets of 3D models. We investigate the lactiferous duct of newborn mice to gain understanding of environmental directed branching. We consider that the lactiferous duct has an innate blue-print of its arborization and assume this blue-print is kind of encoded in an innate L-system. We analyze the duct as it is exposed to different environmental conditions and reflect on the effect on the innate L-system. In order to make sure we can extract the branch structure in the right manner we analyze 3D models of the zebrafish embryo; these are simpler compared to the lactiferous duct and will ensure us that measuring features can result in the separation of different treatments on the basis of differences in the phenotype.

Our system can deal with the complex 3D models, the features separate the experimental conditions. The results provide a means to reflect on the manipulation of an L-system through external factors.

**Keywords:** biological model, 3D reconstruction, phenotype measurement, L-System.

## 1 Introduction

In recent studies [13, 15, 21] three-dimensional (3D) morphological information is used to find the various phenotypes in a sample population. Here the sample population consists of objects in the size range that requires microscope to study them; the differences in the population are found in the micro-anatomy. It is clear that 3D models derived from microscope images potentially offer new insights for analysis. Therefore, 3D images and 3D models are used more frequently over the past years. With image acquisition techniques in bright field microscopy and confocal microscopy it is possible to obtain 3D information from a stack of 2D slices. The sampling is realized by physical sections that are acquired to section images or by optical sections provided by the confocal microscope. The physical section technique is very suitable for modeling histological information whereas the confocal technique is more geared towards imaging specific structures.

From the 3D stack of images a model is derived by segmentation or manual delineation of structures of interest. Manual delineation is used when specific structural knowledge cannot directly be derived from the image; a specialist then selects the specific information through graphical annotation, aka delineation. A set of contours as extracted from the stack subsequently represents the 3D model. The general observation is that the output stack of 2D contours is (nearly) always under sampled perpendicular to the direction of sampling. In order to improve the model, an interpolation can be applied. The classical way of performing such interpolation between section images (slices) is an interpolation of the gray values in the slices so as to estimate the gray values in the missing slices [7]. A linear interpolation for estimating the missing slices, however, may lead to artifacts. A more advanced manner is a shape-based interpolation [7] which is applied directly to the contours of the model.

Techniques of 3D shape reconstruction from consecutive contours fall into two categories: contour stitching and volumetric methods. Contour stitching methods directly connect the vertices of adjacent contours and produce a mesh that passes through all contours such as the methods provided by Keppel [10] and Boissonnat [3]. The volumetric methods first interpolate intermediate gray-values and extract the iso-surfaces from a volumetric field. Representative methods are described by Levin [11], Barrett et al. [2] and Nilsson et al. [16]. Contour based reconstruction methods rely on the fact that the data is organized in parallel planes and performs best on contours that are closed. We tackle the problem of surface reconstruction in a more general way using a point cloud based surface reconstruction method. The merit of a point cloud based reconstruction method is that an abstraction from a specific case to a general problem sheds light on the critical aspects of the problem [8]. Our review paper provides an analytical evaluation of point cloud based reconstruction methods in order to find a method that can reconstruct the surface and suppress the noise with the information from three directions (xyz) [5]. The result of the evaluation shows that the Poisson reconstruction method fits the needs best. As a result, we develop a pipeline to firstly create a uniformly distributed point cloud from a set of plane-parallel contours through shape-based interpolation, then produce a precise and smooth

surface using Poisson reconstruction method and finally extract important surface features to analyze the model that is derived from sampling under different conditions.

Once we have obtained an optimized model we can reduce it to a formalized system. To that end we investigate the connection from a arbor-like structure to a L-system [19, 20] and reason over the phenotypical effects as a result of different conditions to which the subjects are exposed. The remainder of this paper is structured as follows. In section 2 we introduce our methodology. In section 3 we first verify our method with a case study: the zebrafish embryo and subsequently continue with the analysis of the mouse lactiferous duct. In section 4 we present our conclusions and discuss the results.

## 2 Methodology for Model Optimization

Our pipeline is divided into several steps as schematically shown in Figure 1: i.e., (1) contour interpolation, (2) 3D surface reconstruction and (3) phenotype analysis. Subsequent to acquisition, the data are organized in a database and, structures apparent in the images are delineated by a contour. This is done either via segmentation or via a manual delineation for each slice using our dedicated annotation software (TDR); for manual delineation a WACOM digitizer tablet (WACOM, Cintiq LCD-tablet) is used. The contour stacks that are the basis of our models are well aligned by procedures prior to the modeling and in case of the confocal images the alignment is an intrinsic quality of the microscope. In our pipeline we use the stack of images with only the contours as input.

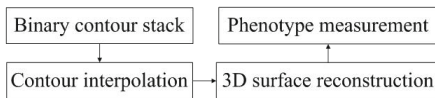


**Fig. 1.** Pipeline of our system

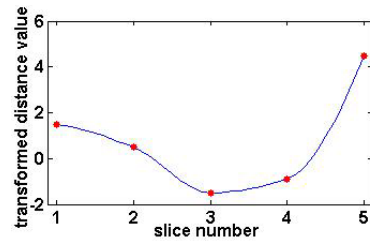


**Fig. 2.** Piecewise cubic Hermite interpolation

### 2.1 Contour Interpolation

For interpolation we make use of a shape-based contour interpolation method. To that end a distance transform is applied in the contour; each point in the resulting image represents the shortest distance to the contour. The points on the contour are zero. Now, the distances inside the contour are positive whereas the distances outside the contour are multiplied with -1 and thus these have a negative value. For each pixel-column in the z-direction, a 1D monotone piecewise

cubic spline [6] is constructed to interpolate distance values in z-direction [4]. In Figure 2 an example for the construction of a 1D-interpolation in z-direction is shown. The reason to use the monotone piecewise cubic spline is that the output spline preserves the shape of the data and at the same time respects monotonicity. In this manner unwanted overshooting artifacts are eliminated by the method. Once the spline is constructed from each vertical column, the intensity of intermediate missing slices at the same column can be evaluated by providing different position values in the z-direction. Finally, the interpolated contour is extracted by setting the threshold of gray-value to zero for each slice. This approach results in an interpolated and equidistant sampled boundary for the model.

## 2.2 3D Surface Reconstruction

In order to be able to use the point cloud based reconstruction method, stack of binary contour images needs to be converted into point cloud in 3D space. Each pixel is converted to a point in 3D space taking the corresponding z-position of the slice into consideration. In this manner the point cloud is created without losing any details and at the same time is indisputably oversampled. From an evaluation of point cloud based reconstruction methods [5] that we conducted previously, we concluded that the Poisson reconstruction method [9] performs the best for both shape preservation and noise suppression. The Poisson reconstruction method, however, requires an oriented point cloud as an input. This means the method needs not only the location but also the normal of each point in the point cloud data. Therefore the normal for each point in the point cloud data is calculated using Hoppe's algorithm [8]. With the oriented point cloud data, the Poisson reconstruction method is applied to create a precise and smooth surface for the model. In necessary, the resolution of the resulting surface model can be tuned by changing the scale parameter which is part of the Poisson reconstruction method.

## 2.3 Phenotype Measurement

The type of measurements extracted from the 3D model strongly depends on the model at hand and the hypothesis posed to resolve phenotypical differences. We extract a range of different features, ones are derived directly from surface including global shape, i.e. volume and surface area, and local features such as surface curvature per point. Other features are extracted from a graph, i.e. skeleton and centerline. These features encode geometrical and topological shape properties in a faithful and intuitive manner [1]. The centerline is useful to describe the topology information of tubular structures such as blood vessels. We notice the L-systems are potentially embedded arbor-like lactiferous duct system. However, the morphological variation of the duct system is regulated by the hormones alteration. With these observations, we conduct the phenotype measurement by extracting the centerline from this arbor-like system. The centerline is a special case of the skeleton which have been studied extensively [12].

The skeleton is the basic representation of the L-system structure. Therefore, the features calculated from the centerline are representative for the arbor-like structure description. These features include number of branches, average branch-length, number of bifurcations, and so on. We would make use of these features for our phenotype analysis.

### 3 Result

The result of surface reconstruction method is used for the shape analysis. We will illustrate this with two different data sets; one from zebrafish and one from mouse development.

#### 3.1 Case Study 1: Zebrafish Embryo, Measurement Verification

First we want to illustrate that the surface reconstruction process can be very well applied to a stack of images. As a test data set, confocal image stacks of zebrafish embryos are used. The images are part of an experiment that consists of two treatments and therefore two different groups; i.e., a control group that develops under normal oxygen levels and a treatment group that develops under a hypoxia condition. For each stack a 3D model of the embryo is constructed by extracting embryo contour per slice. In total the set consists of 21 embryo models (14 with normal treatment, 7 with hypoxia treatment). In Figure 3(a) and (b) the embryo models with different treatment are shown. For each model we calculated the surface area and the volume. The result from the point-cloud reconstruction is a triangulated surface and the surface area is computed by integration over all the triangle patches on the surface. The volume is calculated directly from the mesh using a known method [25]. For an objective assessment of the differences between two treatments, we use sphericity [24] as shape descriptor, described as follows:

$$\Psi = \frac{\pi^{\frac{1}{3}}(6V)^{\frac{2}{3}}}{A} \quad (1)$$

where  $V$  represents the volume of the object and  $A$  represents the surface area of the object. The sphericity is a normalized shape descriptor and for a sphere it equals 1. The higher the sphericity of the object the more it resembles a perfect sphere. Sphericity is computed for all our models and thus mean and standard deviation of the set are available. The results are listed in Figure 3(c). To test for differences, the Kolmogorov-Smirnov Test (KS-test) is used [14]. The test results indicate that sphericity of the control group is significantly smaller than that of hypoxia group. This is consistent with the biology; the hypothesis states that the embryo under normal level of oxygen is developing much faster than the one with hypoxia. As a result the embryo develops uneven in different directions and cannot resemble the spherical shape that it started from. The development of embryo with hypoxia, however, is restrained by the lack of oxygen and the shape remains spherical for a longer time.

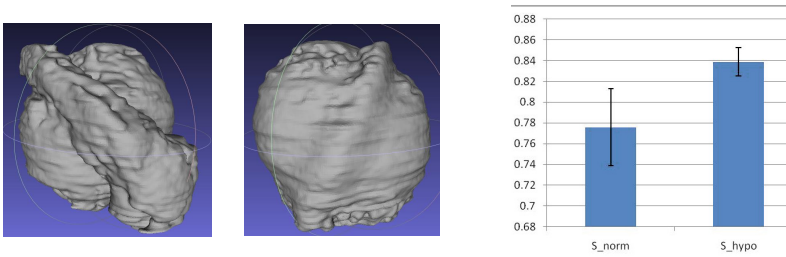


**Fig. 3.** Results of Zebrafish embryo (a) Normal condition (b) Hypoxia condition (c) Sphericity plot

### 3.2 Case Study 2: Mouse Lactiferous Duct, Phenotype Analysis

For our main focus, we shift to topological shape description. We have obtained experimental data from the development of the lactiferous duct; in early development a mouse embryo is exposed to different environmental factors. These factors are hormones or hormone-like substances, a.k.a. endocrine disruptors, and these factors will alter the structure of the duct. This means the innate coding of the L-system is altered and it will result in a different structure or phenotype. We measure the phenotype in order to show the effect of the environmental factor and at the same time we can reason from the result how the L-system is affected. Our study is based on 3D model of the lactiferous duct of newborn mice.

The 3D models are obtained from serial sections with a bright field microscope imaging setup. The images of the lactiferous duct are acquired and a stack of aligned images is used as input for the 3D model [22, 23]. For each stack the lactiferous duct structures are delineated by a specialist resulting in initial 3D models. In the data set used here we included 4 different conditions; meaning that the mother was exposed to these conditions and we would like to measure a maternal effect in the offspring. The control group is not exposed (WT) and consists of 7 models. A condition control group as shown in Figure 5(c),(d) is exposed to an inert component (OLIE) and consists of 12 models. One group is exposed to a specific concentration of diethylstilbestrol (DES) and consists of 8 models. And one group is exposed to a cocktail of estrogen and progesterone (EP) shown in Figure 5(a),(b) and consists of 8 models. From the reconstruction it shows that the mouse lactiferous duct has distinct tree-like structure as depicted in Figure 4. To assess the topological shape differences in the models we will derive the centerline of the lactiferous duct structure, subsequently the arborized structure is used in the analysis. To derive the topological structure a known centerline extraction method is used [17]. These centerlines are the basis of the L-system representation.

For all models interpolation (cf. 2.1) and surface reconstruction (cf. 2.2) is applied. Subsequently, the centerlines of all branches in the arbor-like structure are extracted. For each of the models from each global centerline we extract

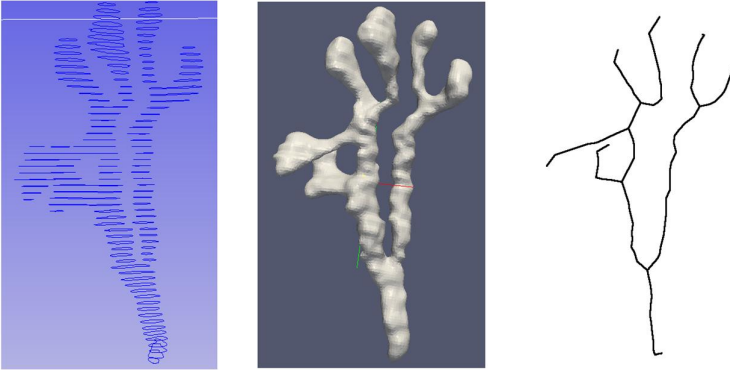


**Fig. 4.** (a) original contour sections; (b) surface model; (c) centerline

**Table 1.** Result of comparison

		length	curvature	torsion	tortuosity	min-radius	max-radius	mean-radius	median-radius
DES-EP	h	0	-1	0	0	0	0	0	0
	p	0.2027	0.0098	0.5588	0.8170	0.7951	0.6364	0.8275	0.9412
OLIE-WT	h	0	0	0	0	0	0	0	0
	p	0.2564	0.8537	0.7724	0.9246	0.0416	0.2951	0.1581	0.3943
DE-OW	h	-1	1	0	0	0	-1	-1	-1
	p	0.0043	0.0031	0.2714	0.5649	0.1007	4.99E-5	0.0026	0.0040

individual branches. For each branch we calculate phenotype measurements including branch length, curvature, torsion, tortuosity, minimal radius, maximal radius, mean of the radius and median of the radius. The curvature of a branch is defined as the average of curvatures of each of the branch-point. The curvature of a point is the inverse of the radius of the local osculating circle. The torsion is the degree by which the osculating plane rotates along the line [18]. The tortuosity is the ratio between the branch length and the distance of the branch endpoints. The radius is defined as the radius of maximum inscribed sphere for each point.

For analysis we construct a dataset by collecting all the branches with measurements from the same group and use the KS-test to check significant differences for every measurement. The hypothesis is that DES and EP will have an effect on the development of the lactiferous duct; this effect should not be seen in the OLIE and WT group in which development should not be affected at all. Consequently, the DES and EP group should be similar and so are the OLIE and WT group. At the same time, the DES and the EP should be significantly different from the OLIE and WT group. We therefore employ the kstest to compare three groups: one between the groups DES and EP (DES-EP); one between the groups OLIE and WT (OLIE-WT); the other one between the combined groups

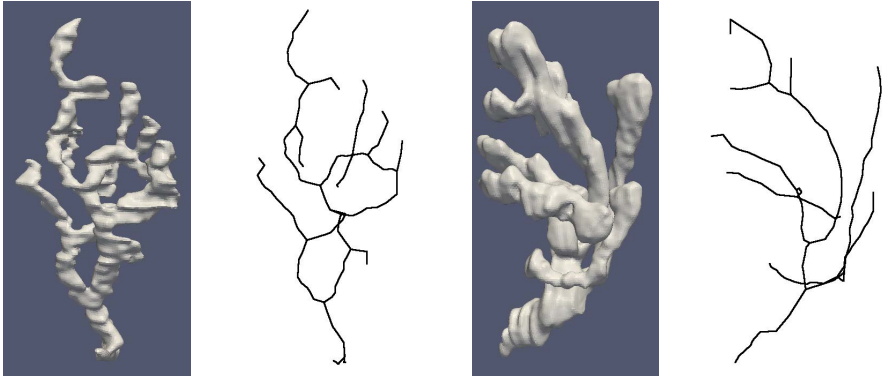


**Fig. 5.** Different branch structures of lactiferous duct (a) surface model from group EP; (b) centerline of the model from group EP; (c) surface model from group OLIE; (d) centerline of the model from group OLIE

DES with EP and OLIE with WT (DE-OW). In Table 1 the results are shown. The p-value refers to the significance level. Value h is 1 if the first dataset is significantly larger than the second. Value h is -1 if the first dataset is significantly smaller than the second dataset. Otherwise, value h is 0. The significance level was set to  $p = 0.01$ . From the results we can see group OLIE and WT are exactly the same. Group DES and group EP are almost the same except for curvature. Nevertheless, the combined group DES with EP and group OLIE with WT are significantly different in length, curvature, maximal radius, mean of the radius and median of the radius. These features seem to be prominent features over torsion, tortuosity and minimal radius. The results accept the hypothesis and also confirm the feasibility of our 3D analysis for such complex system.

## 4 Discussion and Conclusion

In this paper, we introduce a system for 3D representation and analysis from stack of images through a 3D model representation that is derived from that stack. The 3D model needs to be optimized and to that end a point cloud based reconstruction method is used. In this manner the stack of contours in the model is efficiently converted into a uniformly distributed point cloud in 3D space. As such it changes a specific contour based reconstruction problem to a much more generalized point cloud based reconstruction method. Since we take all the 3D points at once to construct the surface representation it makes full use of the boundary point cloud relationship in 3D space. In this way we overcome the restriction imposed by the stack of contours which does not efficiently use the relationship in the z-direction. From our former results we have learned that the Poisson reconstruction method performs well in both shape preserving and noise suppression. This is again confirmed in this current study.



Our purpose is representation and analysis of 3D biological models. The analysis pipeline presented here combines all best techniques and brings us close to realization. The pipeline is applicable to different kinds of dataset that originate from different microscopes and sampling conditions. The complexity that one finds in micro-anatomy can be well covered by the pipeline. Henceforward, we will continue to develop this pipeline and include more techniques in order to be able to deal with the large variation of experimental settings and imaging typical for bio-medical research. The potential of our system in dealing with shape related studies in biology should be explored further.

The 3D models were used for different purposes. The zebrafish embryo models have been used to obtain information on the efficiency of our basic measurements. The lactiferous duct models were used to extract more complex features. In order to accommodate the branching structure that we analyze in a formal structure we invoke the L-system. This nature inspired formal system can help in the understanding of the branching; in fact, we consider an L-system to embody the blue-print of the normal development of the branching duct. Our experimental results illustrate the change of the L-system under environmental conditions and the features we have derived represent the change in phenotype. At the same time the features represent the mutations in the L-system. Thus, this analysis of induced phenotypes helps us in bringing new inspiration to the manipulation of the L-system in which the features provide a quantifiable twist to this system. Our research will be directed in this delicate interplay of nature inspired systems and nature driven models.

**Acknowledgements.** We would like to thank Dr F. Lemmen, J. Korving and W. Hage for their contribution in producing the initial 3D models. This work has been partially supported by the Chinese Scholarship Council and BSIK (Cyttron Project).

## References

1. Akgül, C.B., Sankur, B., Yemez, Y., Schmitt, F.: 3D Model Retrieval Using Probability Density-Based Shape Descriptors. *IEEE Trans. Pattern Anal. Mach. Intell.* 31(6), 1117–1133 (2009)
2. Barrett, W., Mortensen, E., Taylor, D.: An Image Space Algorithm for Morphological Contour Interpolation. In: *Proc. Graphics Interface*, pp. 16–24 (1994)
3. Boissonnat, J.-D.: Shape reconstruction from planar cross sections. *Comput. Vision Graph. Image Process.* 44(1), 1–29 (1988)
4. Braude, I., Marker, J., Museth, K., Nissanov, J., Breen, D.: Contour-based surface reconstruction using implicit curve fitting, and distance field filtering and interpolation. In: *Proc. International Workshop on Volume Graphics*, pp. 95–102 (2006)
5. Cao, L., Verbeek, F.J.: Evaluation of algorithms for point cloud surface reconstruction through the analysis of shape parameters. In: *Proceedings SPIE: 3D Image Processing (3DIP) and Applications 2012*, pp. 82900G–82900G–10. SPIE Bellingham, WA (2012)
6. Fritsch, F.N., Carlson, R.E.: Monotone Piecewise Cubic Interpolation. *SIAM Journal on Numerical Analysis* 17(2), 238–246 (1980)

7. Herman, G.T., Zheng, J., Bucholtz, C.A.: Shape-Based Interpolation. *IEEE Comput. Graph. Appl.* 12(3), 69–79 (1992)
8. Hoppe, H., DeRose, T., Duchamp, T., McDonald, J., Stuetzle, W.: Surface reconstruction from unorganized points. *SIGGRAPH Comput. Graph.* 26(2), 71–78 (1992)
9. Kazhdan, M., Bolitho, M., Hoppe, H.: Poisson surface reconstruction. In: *SGP 2006: Proceedings of the Fourth Eurographics Symposium on Geometry Processing*, Aire-la-Ville, Switzerland, Switzerland, pp. 61–70. Eurographics Association (2006)
10. Keppel, E.: Approximating complex surfaces by triangulation of contour lines. *IBM J. Res. Dev.* 19(1), 2–11 (1975)
11. Levin, D.: Multidimen. In: *Algorithms for Approximation*, pp. 421–431. Clarendon Press, New York (1987)
12. Liu, J., Subramanian, K.: Accurate and robust centerline extraction from tubular structures in medical images 251, 139–162 (2009)
13. Long, F., Zhou, J., Peng, H.: Visualization and analysis of 3D microscopic images. *PLoS Computational Biology* 8(6), e1002519 (2012)
14. Massey, F.J.: The {K}olmogorov- $\{S\}$ mirnov Test for Goodness of Fit. *Journal of the American Statistical Association* 46(253), 68–78 (1951)
15. Ng, A., Brock, K.K., Sharpe, M.B., Moseley, J.L., Craig, T., Hodgson, D.C.: Individualized 3D reconstruction of normal tissue dose for patients with long-term follow-up: a step toward understanding dose risk for late toxicity. *International Journal of Radiation Oncology, Biology, Physics* 84(4), e557–e563 (2012)
16. Nilsson, O., Breen, D.E., Museth, K.: Surface Reconstruction Via Contour Metamorphosis: An Eulerian Approach With Lagrangian Particle Tracking. In: *16th IEEE Visualization Conference (VIS 2005)*, October 23–28. IEEE Computer Society, Minneapolis (2005)
17. Piccinelli, M., Veneziani, A., Steinman, D.A., Remuzzi, A., Antiga, L.: A Framework for Geometric Analysis of Vascular Structures: Application to Cerebral Aneurysms. *IEEE Trans. Med. Imaging* 28(8), 1141–1155 (2009)
18. Pressley, A.: *Elementary differential geometry*. Springer, London (2010)
19. Rozenberg, G., Salomaa, A. (eds.): *The book of L*. Springer-Verlag New York, Inc., New York (1986)
20. Rozenberg, G., Salomaa, A.: *Mathematical Theory of L Systems*. Academic Press, Inc., Orlando (1980)
21. Rübél, O., Weber, G.H., Huang, M.-Y., Wes Bethel, E., Biggin, M.D., Fowlkes, C.C., Luengo Hendriks, C.L., Keränen, S.V.E., Eisen, M.B., Knowles, D.W., Malik, J., Hagen, H., Hamann, B.: Integrating data clustering and visualization for the analysis of 3D gene expression data. *IEEE/ACM Transactions on Computational Biology and Bioinformatics/IEEE* 7(1), 64–79 (2010)
22. Verbeek, F.J., Huijsmans, D.P.: A graphical database for 3D reconstruction supporting (4) different geometrical representations 465, 117–144 (1998)
23. Verbeek, F.J., Huijsmans, D.P., Baeten, R.J.A.M., Schoutsen, N.J.C., Lamers, W.H.: Design and implementation of a database and program for 3D reconstruction from serial sections: A data-driven approach. *Microscopy Research and Technique* 30(6), 496–512 (1995)
24. Wadell, H.: Volume, shape, and roundness of quartz particles. *The Journal of Geology* 43(3), 250–280 (1935)
25. Zhang, C., Chen, T.: Efficient Feature Extraction for 2D/3D Objects in Mesh Representation. In: *Mesh Representation* &quot;, *ICIP 2001*, pp. 935–938 (2001)